JACS
JOURNAL OF THE AMERICAN CHEMICAL SOCIETY

Article

pubs.acs.org/JACS

Effect of Solvent Polarity and Electrophilicity on Quantum Yields and Solvatochromic Shifts of Single-Walled Carbon Nanotube Photoluminescence

Brian A. Larsen,[†] Pravas Deria,[‡] Josh M. Holt,[†] Ian N. Stanton,[‡] Michael J. Heben,[§] Michael J. Therien,[‡] and Jeffrey L. Blackburn*[,†]

[†]Chemical & Materials Science Center, National Renewable Energy Laboratory, 1617 Cole Boulevard, Golden, Colorado 80401, United States

[‡]Department of Chemistry, French Family Science Center, Duke University, 124 Science Drive, Durham, North Carolina 27708, United States

[§]Department of Physics and Astronomy, Wright Center for Photovoltaics Innovation and Commercialization, The University of Toledo, Toledo, Ohio 43606, United States

Supporting Information

ABSTRACT: In this work, we investigate the impact of the solvation environment on single-walled carbon nanotube (SWCNT) photoluminescence quantum yield and optical transition energies (E_{ii}) using a highly charged aryleneethynylene polymer. This novel surfactant produces dispersions in a variety of polar solvents having a wide range of dielectric constants (methanol, dimethyl sulfoxide, aqueous dimethylformamide, and deuterium oxide). Because a common surfactant can be used while maintaining a constant SWCNT−surfactant morphology, we are able to straightforwardly evaluate the impact of the solvation environment upon SWCNT optical properties. We find that (i) the SWCNT quantum yield is strongly dependent on both the polarity and electrophilicity of the solvent and (ii) solvatochromic shifts correlate with the extent of SWCNT solvation. These findings provide a deeper understanding of the environmental dependence of SWCNT excitonic properties and underscore that the solvent provides a tool with which to modulate SWCNT electronic and optical properties.

INTRODUCTION

Single-walled carbon nanotubes (SWCNTs) possess optical transitions in the visible and near-infrared regions of the solar spectrum with energies (E_{ii}) determined by their diameter and chiral angle.[1] These excitonic transitions enable potential applications of SWCNTs in photovoltaics,[2−5] light-emitting diodes,[6] and nanoscale sensors.[7] Integration of SWCNTs into such optoelectronic devices requires a fundamental understanding of excitonic transition energies,[8] diffusion lengths,[9] lifetimes,[3] binding energies,[10,11] recombination mechanisms,[12,13] and luminescence quantum yields.[14−16] For nearly a decade now, photoluminescence excitation (PLE) spectroscopy has been recognized as a powerful tool for characterizing excitonic processes in SWCNTs. In the seminal work by Weisman and Bachilo, PLE spectroscopy of aqueous SWCNT suspensions was performed using sodium dodecyl sulfate (SDS) as a surfactant and the E_{ii} optical transitions of the specific (n,m) species were assigned.[1] It was soon recognized that the optical transition energies, and their corresponding photoluminescence (PL) intensities, depended sensitively on the surrounding dielectric environment,[17,18] as expected for a nanomaterial having all atoms lying on the surface and able to interact intimately with the surroundings.

Since this early work, several studies have investigated the effects of the surrounding surfactant and solvent on the luminescence energies and quantum yields.[8,19−21] Choi and Strano recognized the environmental dependence of optical transition energies as a solvatochromic effect and developed a semiempirical model for comparing the solvatochromic shifts of several SWCNT−surfactant/solvent systems, including SWCNTs in *N*-methyl-2-pyrrolidone and aqueous SWCNT dispersions that employed DNA, SDS, and sodium cholate surfactants.[8] The analysis showed that the observed SWCNT spectral shifts resulted from differences in the medium-dependent exciton polarizability and that the magnitude of the shifts reflected an inverse dependence of exciton polarizability on the diameter and the square of the transition energy. The investigation was limited primarily to aqueous surfactants due to the lack of nonaqueous solvent/surfactant systems capable of producing stable SWCNT dispersions at the time of the study. Consequently, the range over which the dielectric constant could be varied was limited. Instead, the local dielectric environment was perturbed by using different surfactants, which opens the possibility of introducing confounding effects associated with differences in surfactant packing.[22] In an effort to overcome these limitations, Ohno et al. measured the luminescence from SWCNTs suspended across microfabricated trenches immersed in various organic solvents.[19] While this method eliminated surfactant effects and,

Received: December 7, 2011
Published: June 29, 2012

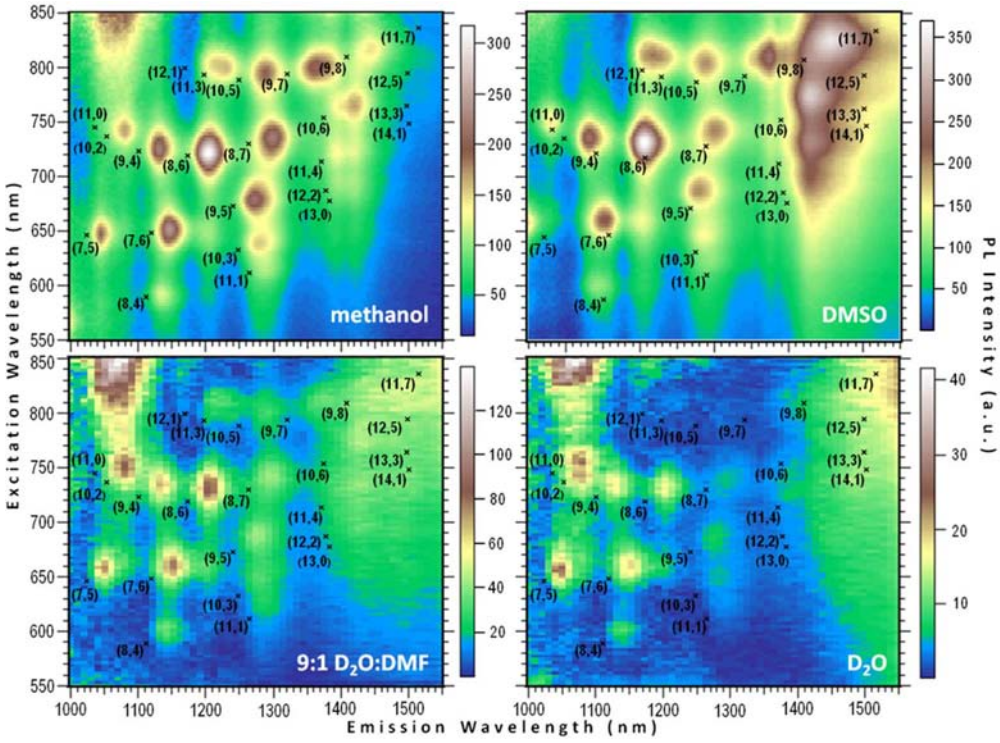

Figure 1. Two-dimensional PLE contour plots of PNES–SWCNTs in methanol, DMSO, 9:1 D_2O/DMF, and D_2O. For reference, the SWCNT(n,m) E_{ii} transition energies from the seminal study by Weisman et al.[1] are also shown on each PLE contour plot, labeled by "×". Experimental conditions: E_{22} spectral region optical density (OD) ~0.5, PLE measured using a front-face detection configuration, T = 25 °C.

in principle, allowed access to a wider range of dielectric constants, the experimental configuration introduced the potential for substrate-induced mechanical strain to impact the measured excitonic transition energies.[23] Other efforts to probe the effect of the environment on SWCNT excitonic properties include studies by Ju et al.[15] and Silvera-Batista et al.[20] in which SWCNTs were exposed to organic solvents; Silvera-Batista et al., for example, introduced nonaqueous solvent species into the nonpolar "microenvironment" within micelles that encapsulated and suspended nanotubes in aqueous solution. These studies, however, were naturally limited to low dielectric constant, nonpolar solvents.

To more completely understand the role of solvent/SWCNT interactions on the PL quantum yield (QY) and optical transition energies (E_{ii}), we used a novel, highly charged, aryleneethynylene polymer[24−26] as a surfactant. Previous work demonstrated that ionic poly[1,5-bis(3-propoxysulfonic acid sodium salt)-2,6-naphthylene]ethynylene (PNES) exfoliates, individualizes, and disperses SWCNTs in both water and organic solvents such as DMSO (dimethyl sulfoxide), DMF (dimethylformamide), and MeOH (methanol) via a single-chain wrapping mechanism.[25] Atomic force microscopy (AFM) and transmission electron microscopy (TEM) data highlighted that PNES wraps SWCNTs with a helix pitch length of 10 ± 2 nm while retaining a constant morphology in a wide range of solvents. (Characterization of the SWNT–PNES conformation is available in the Supporting Information (S-1).) Thus, PNES permits SWCNT solvatochromism to be studied in solvents having a wide range of dielectric constants while the surfactant structure surrounding the nanotube is fixed. This approach enables straightforward evaluation of the impact of solvation environment on SWCNT optical properties and provides a deeper understanding of the environmental dependence of SWCNT excitonic states.

We report PLE spectroscopy data for PNES-dispersed SWCNTs in various polar solvents [methanol, DMSO, aqueous DMF (9:1 D_2O/DMF), and deuterium oxide (D_2O)]. We find that the SWCNT PL QY is strongly dependent on the solvent polarity, decreasing by an order of magnitude in D_2O, a high dielectric solvent, relative to that observed in a less polar solvent such as DMSO. We also find that the PL QY and solvatochromic shifts are remarkably similar in methanol and DMSO despite the large difference between their respective dielectric constants. Further analysis of these results reveals that, in addition to solvent polarity, the PL QY is dependent on the electrophilic character of the solvent, while the solvatochromic shifts correlate with the extent of SWCNT solvation.

■ RESULTS AND DISCUSSION

Photoluminescence spectra were obtained as a function of excitation wavelength to generate two-dimensional PLE contour plots of each PNES–SWCNT solution (Figure 1), as described previously.[27] The PLE spectra of PNES–SWCNTs in all solvents are consistent with individualized unbundled SWCNTs in solution, with well-defined peaks for the various (n,m) SWCNT species and negligible Forster resonant energy transfer from large to small band gap SWCNTs. All PNES–SWCNT/solvent samples were diluted to a similar optical density (OD) of ~0.5 in the E_{22} spectral region; PLE measurements were made with a 1 cm path length cuvette using a front-face detection configuration to minimize inner-filter effects from solvent absorption. (Optical absorbance spectra and further details on the PLE measurements are available in the Supporting Information (S-2).) From the (n,m)

dx.doi.org/10.1021/ja2114618 | J. Am. Chem. Soc. 2012, 134, 12485–12491

species in each of the PLE contour plots, the *relative quantum yield* (Φ_{PL}) was calculated as the ratio of the E_{11} PL intensity to the E_{22} optical density for particular (n,m) species in each PNES−SWCNT/solvent system. In Figure 2a, Φ_{PL} for selected species is plotted as a function of the solvent dielectric constant (ε_s), a common measure of solvent polarity.

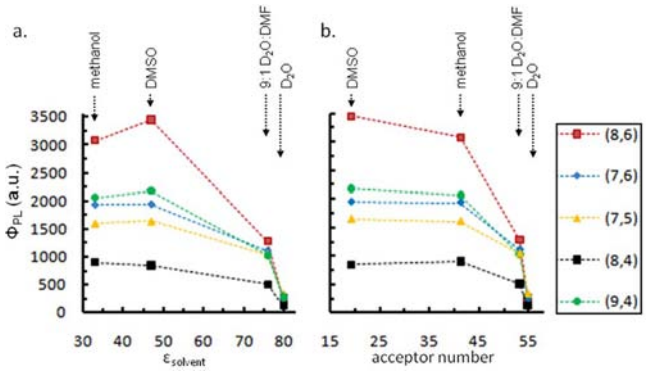

Figure 2. Relative SWCNT PL quantum yields (Φ_{PL}) of (8,6), (7,6), (7,5), (8,4), and (9,4) tubes plotted as a function of the solvent dielectric constant (a) and solvent acceptor number (b). Note that the SWCNT Φ_{PL} decreases in the higher dielectric and more electrophilic solvents, consistent with SWCNT PL quenching via dielectric screening of excitons by solvent molecules. Dashed lines in both plots are guides for the eye, and the measurement error of Φ_{PL} is ∼1.8%.

While relatively high Φ_{PL} values are observed for low dielectric constant solvents such as methanol and DMSO, Φ_{PL} is dramatically lower for the high ε_s environments (e.g., in 9:1 D_2O/DMF and D_2O solvents). The decreased Φ_{PL} with higher ε_s is consistent with results obtained by Silvera-Batista et al.[20] for low dielectric constant solvent species ($2 < \varepsilon_s < 10$) incorporated within SWCNT-encapsulating micelles in aqueous solution. Also, it is interesting to note that other nanoscale systems with excitonic excited states, such as quantum dots[28] and nanostructured porous silicon,[29] exhibit a similar Φ_{PL} dependence on ε_s. In the case of porous silicon, the decreased PL intensity has been attributed to increased dielectric screening of the electron−hole Coulombic interaction by solvent molecules, which reduces radiative exciton recombination in lieu of nonradiative free carrier recombination.[29] While the role of ε_s in SWCNT exciton dynamics is not yet fully understood, a similar enhancement of nonradiative recombination pathways through dielectric screening is a likely source for the inverse relationship observed between the *polarity* of solvents and SWCNT PL intensity.

Further consideration of the results in Figure 2a suggests that the dielectric properties of the solvent alone do not fully predict the SWCNT PL quenching observed in the PNES−SWCNT dispersions. For example, the SWCNT PL is significantly quenched in D_2O relative to 9:1 D_2O/DMF, despite a very small difference in $\varepsilon_{solvent}$ ($\varepsilon_{D_2O} = 80$, $\varepsilon_{9:1\ D2O/DMF} = 76$). While this increased PL in the 9:1 D_2O/DMF compared to D_2O may be caused in part by preferential interaction of DMF molecules with the SWCNT surface,[30,31] it appears that the SWCNT Φ_{PL} is affected by additional solvent interactions not described by the solvent polarity, particularly for DMSO and methanol. Despite the greater polarity of DMSO relative to methanol ($\varepsilon_{DMSO} = 47$, $\varepsilon_{methanol} = 33$), the SWCNT Φ_{PL} is appreciably greater in DMSO (Figure 2a).

Acid-induced PL quenching of aqueous SWCNT solutions is a well-documented phenomenon[12,13,32,33] and is attributed to the electron-withdrawing nature of acidic species. Physically adsorbed protons on the SWCNT surface withdraw electron density from the SWCNT π-system, creating nonradiative recombination sites by electronically modulating ("hole-doping") the SWCNT.[14] While discussion of this electron-withdrawing mechanism is typically limited to the context of protic acid interaction with SWCNTs, it is reasonable to consider that electrophilic solvent molecules may also quench SWCNT PL through related perturbations to the SWCNT π-system electron density. To explore this possibility in more detail, Φ_{PL} was plotted as a function of the solvent acceptor number (Figure 2b). The solvent acceptor number (AN) is a relative measure of the electrophilic character (electrophilicity) of a solvent and is determined by the ^{31}P NMR chemical shift induced by the electron-withdrawing interactions of the solvent with the triethylphosphine oxide oxygen lone pair.[34] Interestingly, plotting the PL data versus AN results in a monotonic trend line, consistent with solvent electrophilicity playing a significant role in SWCNT PL quenching. The quantities plotted in Figure 2 are tabulated in Table 1.

Table 1. Solvent Properties and SWCNT Φ_{PL} in Solution

			SWCNT Φ_{PL}				
solvent	$\varepsilon_{solvent}$	AN	(7,6)	(8,6)	(7,5)	(8,4)	(9,4)
DMSO	47	19.3	1945	3449	1643	846	2178
methanol	33	41.5	1935	3075	1607	905	2060
9:1 D_2O/DMF	76[a]	48.6[b]	1114	1279	1046	510	1025
D_2O	80	54.8	245	252	335	119	280

[a] $\varepsilon_{9:1\ D2O/DMF}$ was estimated by the volume-weighted sum of ε_{DMF} and ε_{D_2O}. [b] $AN_{9:1\ D2O/DMF}$ was estimated by interpolation of DMF/D_2O AN data[37] using a 2.5% DMF molar ratio.

The relationship between the SWCNT Φ_{PL} and solvent AN shown in Figure 2b is the first systematic report demonstrating that, in addition to the well-known mechanism of SWCNT PL quenching by protonation from Brønsted acids, SWCNT PL can also be quenched by aprotic electrophilic solvents. This observation is further supported by plotting the SWCNT Φ_{PL} versus the solvent donor number (DN), which is a relative measure of the electron-donating character (donicity) of a solvent.[34] A comparison of the SWCNT Φ_{PL} and solvent DN demonstrates an inverse relationship with respect to that seen with the solvent AN: The SWCNT Φ_{PL} increases in solvents with greater electron donicity. (For a plot of the SWCNT Φ_{PL} vs solvent DN, see the Supporting Information (S-3).) Our previous SWCNT solid-state NMR studies support the relevance of comparing the solvent AN, determined by ^{31}P NMR, to the solvent-induced PL quenching observed in this study. We have observed ^{13}C chemical shifts of SWCNTs induced by various adsorbed chemical dopants[35,36] that are directly analogous to the ^{31}P chemical shifts used to determine a solvent's AN. These results, which indicate that solvent electrophilicity impacts SWCNT exciton dynamics, underscore that the solvent provides a tool with which to modulate SWCNT excitonic properties. Furthermore, the role of solvent electrophilicity likely provides insight into earlier SWCNT studies that reported anomalous PL quenching results. For example, in the recent SWCNT/solvent PL study by Silvera-Batista et al.,[20] the two solvents with the highest electro-

dx.doi.org/10.1021/ja2114618 | J. Am. Chem. Soc. 2012, 134, 12485−12491

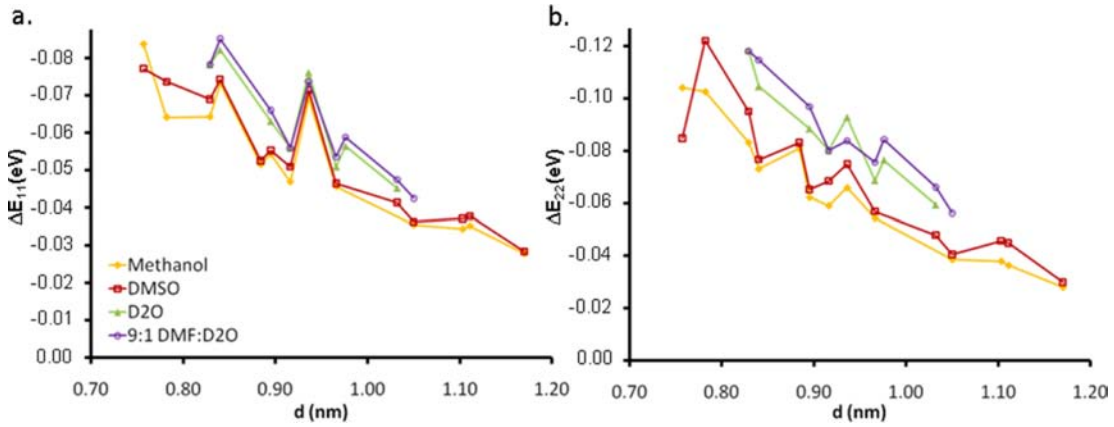

Figure 3. Solvent-dependent bathochromic shifts of the PNES−SWCNT E_{11} emission energies (a) and E_{22} excitation energies (b), shown as a function of the SWNT diameter. All bathochromic shifts are relative to the calculated E_{ii} for SWNTs in vacuum.

philicities, chloroform and 3-heptanol, demonstrated the greatest deviation of the Φ_{PL} versus ε_s trend and displayed significantly lower SWCNT PL intensities relative to solvents possessing similar ε_s values.

In addition to affecting the intensity of the PL, the solvent properties can also influence the SWCNT optical transition energies (E_{ii}). Solvatochromic shifts (ΔE_{ii}) of each PNES−SWCNT/solvent system are displayed in Figure 3 as a function of the SWCNT diameter. Measured solvatochromic shifts are presented relative to E_{ii} values for SWCNTs in vacuum ($E_{ii,vac}$), which were determined using a relationship originally developed by Bachilo et al.[38] and later adapted by Choi and Strano:[8]

$$E_{ii} = \frac{1241}{A_1 + A_2 d} + A_3 \frac{\cos(3\theta)}{d^2} \quad (1)$$

A_1, A_2, and A_3 are parameters determined from published values for E_{ii} in vacuum.[8] (For a detailed description of eq 1, see the Supporting Information (S-4).) θ and d are the chiral angle and diameter, respectively, of each SWCNT(n,m) species. Calculating $E_{ii,vac}$ using eq 1 was necessary due to the lack of published experimental E_{ii} data in vacuum for the SWCNT(n,m) species used in this study. Figure 3 demonstrates (n,m)-specific solvatochromic shifts for each PNES−SWCNT/solvent system, displaying increasing E_{11} and E_{22} bathochromic shifts with decreasing SWCNT diameter. The magnitude and diameter-dependent slope of ΔE_{22} are slightly larger than those of ΔE_{11} for a given solvent. These differences are expected from a consideration of the relative magnitudes of many-body Coulomb interactions (both the repulsive electron−electron self-energy and attractive electron−hole binding energy) for E_{11} and E_{22} excitons,[39] as discussed in detail in the Supporting Information (S5).

Insight into the origin of the SWCNT diameter-dependent solvatochromic shifts of the E_{11} and E_{22} transition energies is obtained by analyzing the data within a model that treats SWCNTs as solutes that may be polarized via the solvent Stark effect. Briefly, the solvent Stark effect[40,41] refers to the solvatochromic shift that arises when a solute is polarized by an external static electric field. The following model is derived (for a derivation of the solvatochromism model in eq 2, see the Supporting Information (S-6)) from a closed-form expression describing the stabilization energy of an induced dipole within a photoexcited SWCNT by the surrounding solvent molecules.[42]

$$\Delta E_{ii} E_{ii,vac}{}^3 = -D_{SWNT/solvent}[f(\varepsilon) - f(\eta^2)]_{solvent} \frac{1}{d^5} \quad (2)$$

Here, ΔE_{ii} is the solvatochromic shift relative to $E_{ii,vac}$ for each SWCNT(n,m) species (vide supra), $D_{SWCNT/solvent}$ describes the SWCNT/solvent interactions and is defined as the product of C_{SWCNT} and $L_{solvent}$ (described below), $[f(\varepsilon) - f(\eta^2)]_{solvent}$ is the difference between the solvent's Onsager polarity functions, which reflects the solvent's polar properties by accounting for both the dipole moment and polarizability of the solvent, and d is the diameter of the Onsager volume in which the solvent molecules interact with the SWCNT, which is assumed to be proportional to the diameter of a particular SWCNT species. The parameter C_{SWCNT} is proportional to the polarizability of a photoexcited SWCNT, and $L_{solvent}$ is associated with solvent interactions with the SWCNT solute and reflects the polarization fluctuation within the Onsager volume. Since ΔE_{ii} is defined relative to the values in vacuum, $[f(\varepsilon) - f(\eta^2)]_{solvent}$ is simply determined by $\varepsilon_{solvent}$ and $\eta_{solvent}$, the static dielectric constant and refractive index of the solvent, respectively. The values for the power coefficients in eq 2 ($E_{ii,vac}{}^3$ and d^{-5}) are taken from the recent work of Silvera-Batista et al., in which the longitudinal polarizability of the SWCNT exciton (α_{ii}) was found to conform to the functional form $\alpha_{ii} \propto d^{-2} E_{ii}{}^{-3}$.[20]

The model described in eq 2 was applied to the ΔE_{ii} PLE data for each PNES−SWCNT/solvent system by plotting $\Delta E_{ii} E_{ii,vac}{}^3$ versus d^{-5} as shown in Figure 4. The high linear correlation coefficients of the dashed lines highlighted in Figure 4 ($R^2 > 0.995$ and 0.972 for the E_{11} and E_{22} data, respectively), suggest that the eq 2 solvatochromism model provides a reasonable framework for analyzing the experimental results. The E_{22} data are slightly less linearly correlated, which may derive in part from the coarse PLE excitation resolution of 3 nm. The linear regression slopes ($-m_{solvent}$) for each PNES−SWCNT/solvent system effectively capture the species-dependent solvatochromic behavior for all luminescent species in the ensemble since $-m_{solvent}$ relates the species-dependent ΔE_{ii} to intrinsic SWCNT properties (d and $E_{ii,vac}$). A greater magnitude of $-m_{solvent}$ represents a greater bathochromic shift of the excitation (E_{22}) and emission (E_{11}) energies for all SWCNTs within a particular PNES−SWCNT ensemble. Thus, using $-m_{solvent}$ as a representative metric for a particular sample's species-dependent solvatochromic behavior, we compare the observed solvatochromic shifts for the emissive E_{11} transitions

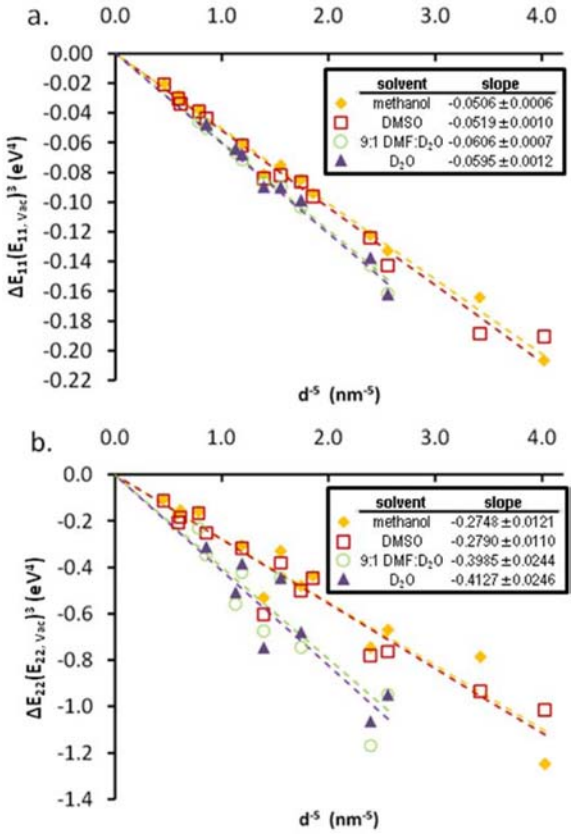

Figure 4. Figure 1 PLE data modeled according to eq 2. E_{11} (emission, a) and E_{22} (excitation, b) bathochromic shifts are relative to the calculated E_{ii} for SWNTs in vacuum ($E_{ii,vac}$). The dashed lines were obtained via linear regression of the data.

of the PNES−SWCNT/solvent systems in greater detail below. The PNES−SWCNT/methanol and PNES−SWCNT/DMSO systems exhibit statistically identical (for a detailed explanation of the linear regression statistical significance, see the Supporting Information (S-7)) species-dependent E_{11} bathochromic shifts relative to that in vacuum: $-m_{methanol}$ = 0.0506 ± 0.0006 and $-m_{DMSO}$ = 0.0519 ± 0.0010 $eV^4 \cdot nm^{-5}$. The slopes $-m_{D_2O}$ and $-m_{9:1\ D_2O/DMF}$ are also statistically indistinguishable ($-m_{D_2O}$ = 0.0595 ± 0.0012 and $-m_{9:1\ D_2O/DMF}$ = 0.0606 ± 0.0007 $eV^4 \cdot nm^{-5}$), but are substantially larger than the slopes obtained for the DMSO and methanol samples.

To understand the solvent dependence of PNES−SWCNT emissive transition energies in more detail, we consider the solvent/solute parameters that should affect the regressed $-m_{solvent}$ values. Returning to eq 2, we see that $-m_{solvent}$ is determined by the product of two terms: (1) the Onsager term, related to the intrinsic solvent properties ($[f(\varepsilon) - f(\eta^2)]$), and (2) an expression capturing the interactions of the SWCNTs with each solvent ($-D_{SWCNT/solvent}$). If one were to consider solvent polarity as the dominant factor affecting the solvatochromic shift, the identical $-m_{solvent}$ values for DMSO and methanol are an unexpected result. Since DMSO is a considerably more polar solvent than methanol, the Onsager term ($[f(\varepsilon) - f(\eta^2)]$) is significantly different for these two solvents. This implies that the solvent−solute interactions, as captured by $-D_{SWCNT/solvent}$, must differ between the two solvents, giving rise to statistically identical bathochromic shifts. Using the linearly regressed $-m_{solvent}$ values from the data shown in Figure 4, we calculate $-D_{SWCNT/solvent}$. The calculated values for $-D_{SWCNT/solvent}$ are shown in Table 2 and differ among the different PNES−SWCNT/solvent systems.

The $-D_{SWCNT/solvent}$ variation (∼21%) observed in this study exceeds the $-D_{SWCNT/solvent}$ variation (∼14%) observed previously by Silvera-Batista et al. (referred to as $D_{solvent}$ in their work), which may be explained by the exclusive use of nonpolar solvents in the former study,[20] in contrast to the range of polar solvents examined here. In nonpolar solvents, the SWCNT/solvent interactions arise from induced dipole−induced dipole (London dispersion) forces, while in polar solvents, these interactions arise from dipole−induced dipole (Debye) forces. The dipole−induced dipole interaction (i.e., the solvent Stark effect) originates from the random motion of solvent dipoles near the SWCNT surface, inducing a dipole moment in the SWCNT.[42] On the basis of the underlying physical mechanisms of this interaction, it follows that the magnitude of the SWCNT solvatochromic shift is strongly related to the degree of SWCNT solvation, as captured by the $-D_{SWCNT/solvent}$ parameter. Since the solvatochromic shift is the electrostatic stabilization energy of the photoexcited SWCNT exciton by solvent molecules, it follows that greater SWCNT solvation implies stronger Debye interactions at the SWCNT/solvent interface, resulting in a greater stabilization energy. In this context, $-D_{SWCNT/solvent}$ represents the magnitude of the solvatochromic interaction between the SWCNT and solvent, as $-D_{SWCNT/solvent}$ normalizes the observed solvatochromic shift of each SWCNT/solvent system by the intrinsic polarities of each solvent.

To better understand the origin of the observed differences for $-D_{SWCNT/solvent}$ in Table 2, we recall from eq 2 that $-D_{SWCNT/solvent}$ is the product of $L_{solvent}$ and C_{SWCNT}. Since C_{SWCNT} is related to the polarizability of a photoexcited SWCNT and is thus an intrinsic SWCNT parameter, it follows that the observed differences in $-D_{SWCNT/solvent}$ must depend on $L_{solvent}$, a parameter associated with the interaction of the polar solvent molecules with the polarizable photoexcited SWCNTs in solution. To explore the solvent physical properties with which $-D_{SWCNT/solvent}$ may correlate, we narrow our consideration to solvent parameters associated with

Table 2. Linearly Regressed Solvatochromic Shifts of PNES−SWCNT/Solvent Samples and Solvent Parameters[a]

solvent	$-m_{solvent}(E_{11})$ ($eV^4 \cdot nm^{-5}$)	$[f(\varepsilon) - f(\eta^2)]_{solvent}$	$-D_{SWCNT/solvent}$ ($eV^4 \cdot nm^{-5}$)	$\lvert\Delta E_{S,T}\rvert$ (mJ/m^2)	$\Delta\delta_D^2$ (MPa)
methanol	0.0506 ± 0.0006	0.618	0.0819	17	9.61
DMSO	0.0519 ± 0.0010	0.526	0.0987	4	0.36
D_2O	0.0595 ± 0.0012	0.640	0.0930	33	4.84
9:1 D_2O/DMF	0.0606 ± 0.0007	0.632	0.0959	29	4.08

[a] $m_{solvent}(E_{11})$ is the linearly regressed slope of the data shown in Figure 4, $f(\varepsilon)$ and $f(\eta^2)$ are the Onsager polarity functions of the solvent, $D_{SWCNT/solvent}$ is associated with SWCNT/solvent interactions, $\Delta E_{S,T}$ is the difference in surface energy between the SWCNT and solvent, and $\Delta\delta_D$ is the difference in dispersive Hansen solubility parameters (vide infra) between the SWCNT and solvent.

dx.doi.org/10.1021/ja2114618 | J. Am. Chem. Soc. 2012, 134, 12485−12491

SWCNT solvation. Bergin et al. explored various SWCNT/solvent solubility parameters and suggested that the fundamental parameter determining SWCNT solvation is the solvent surface energy,[43] which is the energy required to disrupt the intermolecular bonds of the solvent to create a SWCNT/solvent surface. Specifically, Bergin et al. empirically found that minimization of the surface energy difference, $|\Delta E_{S,T}|$, between the SWCNT and solvent was a reliable predictor for effective SWCNT solvation. We calculated the $|\Delta E_{S,T}|$ for each solvent (Table 2) using 70 mJ/m^2 as an estimate of the SWCNT surface energy[43] and approximating the solvent surface energy as ∼30 mJ/m^2 greater than the solvent surface tension,[44] but found no obvious relationship between $-D_{SWCNT/solvent}$ and $|\Delta E_{S,T}|$.

In addition to $|\Delta E_{S,T}|$, Bergin et al. also observed a strong SWCNT solvation dependence on the dispersive Hansen solubility parameter, δ_D,[43] which is defined by Hansen as the square root of the contribution of London dispersion forces to the cohesive energy density of a solvent.[45] In Table 2, we calculate for each solvent the squared difference between $\delta_{D,SWCNT}$ and $\delta_{D,solvent}$ ($\Delta\delta_D^2$) using $\delta_{D,SWCNT}$ = 17.8 MPa$^{1/2}$ [43] and literature $\delta_{D,solvent}$ data.[45] Similar to $|\Delta E_{S,T}|$, minimizing $\Delta\delta_D^2$ between the solvent and SWCNT predicts strong SWCNT solvation,[43] i.e., strong association of the solvent molecules with the SWCNT surface. Interestingly, we observe a consistent inverse correlation when comparing $-D_{SWCNT/solvent}$ vs $\Delta\delta_D^2$ (Figure 5). This apparent relationship is consistent

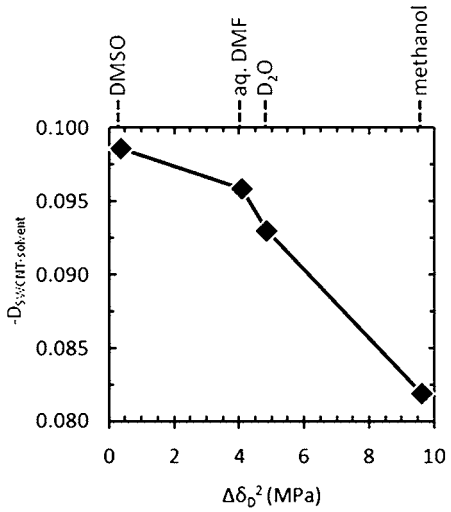

Figure 5. Dependence of $-D_{SWCNT/solvent}$ on $\Delta\delta_D^2$, indicating greater SWCNT interaction with solvent molecules as the difference decreases between dispersive Hansen solubility parameters. The solid line is displayed as a guide for the eye.

with the physical expectation that increased SWCNT solvation (quantified as a minimized $\Delta\delta_D^2$) results in greater SWCNT interaction with the solvent, indicated by an increased value of $-D_{SWCNT/solvent}$. This relationship is consistent among the four PNES−SWCNT/solvent systems in this study and is in agreement with the solvent Stark effect mechanism of SWCNT solvatochromism. On the basis of these results, we conclude that SWCNT solvatochromic shifts are determined not only by solvent polarity, but also by the degree of SWCNT solvation, and that the solvation is best correlated with the dispersive Hansen solubility parameters ($\Delta\delta_D^2$) of the SWCNT and solvent.

CONCLUSION

In conclusion, we have investigated the influence of solvent on the SWCNT quantum yield and solvatochromic shifts in a wide range of polar solvents. Our results indicate that the SWCNT quantum yield is affected by solvent polarity, as represented by the dielectric constant ($\varepsilon_{solvent}$) and also by solvent electrophilicity, quantified by the solvent acceptor number. Considering these two distinct solvent parameters, we propose two separate mechanisms by which solvents with either relatively high polarity or high electrophilic character may quench SWCNT luminescence. Highly polar solvents may quench the SWCNT quantum yield via dielectric screening of excitons by solvent molecules, leading to exciton dissociation and enhanced nonradiative recombination. In the case of electrophilic solvents, the solvent molecules may perturb the SWCNT electron structure by shifting electron density from the nanotube surface, thus creating nonradiative recombination sites, which also reduce the SWCNT quantum yield. The role of solvent electrophilicity has not been explored previously, and the results of this study underscore the need to further investigate the effects of intrinsic solvent properties on SWCNT quantum yield. Our results also indicate that SWCNT solvatochromic shifts are dependent not only on solvent polarity but also on the degree of SWCNT solvation. The nature of SWCNT solvation, and how solvent/SWCNT interactions impact SWCNT absorptive and emissive solvatochromic shifts, has been little interrogated. The advent of highly charged polymers such as PNES, which exfoliate and individualize SWCNTs in multiple solvents via single-chain helical wrapping that maintains a constant PNES−SWCNT morphology regardless of the medium,[25] makes such investigations now possible. Such insights into the environmental dependence of SWCNT excitonic properties will undoubtedly define important design considerations relevant to the development of SWCNT-based electrooptic materials and devices with particular importance for SWCNT applications in complex chemical environments, such as SWCNT biosensing both in vivo and in vitro.[46,47]

MATERIALS AND METHODS

Preparation of PNES−SWCNT Suspensions. All manipulations were carried out under nitrogen prepurified by passage through an O_2 scrubbing tower (Schweizerhall R3-11 catalyst) and a drying tower (Linde 3 Å molecular sieves) unless otherwise noted. Standard Schlenk techniques were employed to manipulate air-sensitive solutions. All solvents utilized in this work were obtained from Fisher Scientific (HPLC grade). HiPco (batch R0539) as-produced SWNTs were obtained from Rice University and used without further purification. 1,4,7,10,13-Pentaoxacyclopentadecane (15-crown-5) was obtained from Aldrich and used as received. PNES−SWCNT suspensions were prepared identically to the method reported previously,[25] save for the modifications that (i) 15-crown-5 was utilized as the phase transfer catalyst instead of the reported 18-crown-6 and (ii) the preparative scale was doubled. In brief, a 5 mL solution of ionic PNES (1.68 mg/mL, $M_n \approx$ 18.8 kDa, degree of polymerization (DP) ∼40, polydispersity index ∼1.11) was sonicated with 4 mg of HipCo (batch R0539) nanotubes in direct contact with a tip horn sonicator (20 kHz) and centrifuged (70000*g* and 3 h for aqueous and 45000*g* and 1 h for organic solvent suspensions). The upper 60% of the supernatant was collected. The preparation of an aqueous suspension involves sonication for 3 h (1 W/mL). Organic suspensions were obtained by dissolving PNES in the desired solvent with the phase transfer catalyst 15-crown-5 (∼10−20 mg/mL; sonication conditions were 1 h and 0.4 W/mL). PNES−SWCNT suspensions were diluted to an OD of 0.5 for PLE by adding an

dx.doi.org/10.1021/ja2114618 | J. Am. Chem. Soc. 2012, 134, 12485−12491

appropriate amount of neat solvent. Added detail (including structural characterization) can be found in an earlier paper.[25]

PLE and Optical Absorbance Spectroscopies. PLE spectra were obtained in a front-face configuration using a modified Fourier transform infrared instrument (Nicolet FT960) with excitation provided by a tungsten lamp coupled to a monochromator. Details of the apparatus are presented elsewhere.[27] Optical absorbance spectra were obtained on a Cary 9600 UV−vis−NIR instrument.

■ ASSOCIATED CONTENT

Ⓢ Supporting Information

Structural and conformation characterization of PNES−SWCNT, optical absorption spectra, further discussion of the results, derivation of analytical expressions, additional description of the methods, and tabulated data. This material is available free of charge via the Internet at http://pubs.acs.org/.

■ AUTHOR INFORMATION

Corresponding Author

Jeffrey.Blackburn@nrel.gov

Notes

The authors declare no competing financial interest.

■ ACKNOWLEDGMENTS

This work was funded by the Solar Photochemistry program of the U.S. Department of Energy, Office of Science, Basic Energy Sciences, Division of Chemical Sciences, Geosciences and Biosciences, under Contract No. DE-AC36-08GO28308 to the National Renewable Energy Laboratory and Grant DE-SC0001517 to M.J.T.

■ REFERENCES

(1) Weisman, R. B.; Bachilo, S. M. *Nano Lett.* **2003**, *3*, 1235−1238.
(2) Ferguson, A. J.; Blackburn, J. L.; Holt, J. M.; Kopidakis, N.; Tenent, R. C.; Barnes, T. M.; Heben, M. J.; Rumbles, G. *J. Phys. Chem. Lett.* **2010**, *1*, 2406−2411.
(3) Holt, J. M.; Ferguson, A. J.; Kopidakis, N.; Larsen, B. A; Bult, J.; Rumbles, G.; Blackburn, J. L. *Nano Lett.* **2010**, *10*, 4627−4633.
(4) Bindl, D. J.; Safron, N. S.; Arnold, M. S. *ACS Nano* **2010**, *4*, 5657−5664.
(5) Ham, M. H.; Paulus, G. L. C.; Lee, C. Y.; Song, C.; Kalantar-Zadeh, K.; Choi, W.; Han, J. H.; Strano, M. S. *ACS Nano* **2010**, *4*, 6251−6259.
(6) Aguirre, C. M.; Auvray, S.; Pigeon, S.; Izquierdo, R.; Desjardins, P.; Martel, R. *Appl. Phys. Lett.* **2006**, *88*, 183104.
(7) Barone, P. W.; Baik, S.; Heller, D. A.; Strano, M. S. *Nat. Mater.* **2005**, *4*, 86−92.
(8) Choi, J. H.; Strano, M. S. *Appl. Phys. Lett.* **2007**, *90*, 223114.
(9) Cognet, L.; Tsyboulski, D. A; Rocha, J. D. R.; Doyle, C. D.; Tour, J. M.; Weisman, R. B. *Science* **2007**, *316*, 1465−1468.
(10) Dukovic, G.; Wang, F.; Song, D.; Sfeir, M. Y.; Heinz, T. F.; Brus, L. E. *Nano Lett.* **2005**, *5*, 2314−2318.
(11) Ma, Y. Z.; Valkunas, L.; Bachilo, S. M.; Fleming, G. R. *J. Phys. Chem. B* **2005**, *109*, 15671−15674.
(12) Blackburn, J. L.; McDonald, T. J.; Metzger, W. K.; Engtrakul, C.; Rumbles, G.; Heben, M. J. *Nano Lett.* **2008**, *8*, 1047−1054.
(13) Dukovic, G.; White, B. E.; Zhou, Z.; Wang, F.; Jockusch, S.; Steigerwald, M. L.; Heinz, T. F.; Friesner, R. A.; Turro, N. J.; Brus, L. E. *J. Am. Chem. Soc.* **2004**, *126*, 15269−12576.
(14) Wang, F.; Dukovic, G.; Knoesel, E.; Brus, L.; Heinz, T. *Phys. Rev. B* **2004**, *70*, 1−4.
(15) Ju, S. Y.; Kopcha, W. P.; Papadimitrakopoulos, F. *Science* **2009**, *323*, 1319−1323.
(16) Metzger, W. K.; McDonald, T. J.; Engtrakul, C.; Blackburn, J. L.; Scholes, G. D.; Rumbles, G.; Heben, M. J. *J. Phys. Chem. C* **2007**, *111*, 3601−3606.
(17) Perebeinos, V.; Tersoff, J.; Avouris, P. *Phys. Rev. Lett.* **2004**, *92*, 8−11.
(18) Strano, M. S.; Moore, V. C.; Miller, M. K.; Allen, M. J.; Haroz, E. H.; Kittrell, C.; Hauge, R. H.; Smalley, R. E. *J. Nanosci. Nanotechnol.* **2003**, *3*, 81−86.
(19) Ohno, Y.; Iwasaki, S.; Murakami, Y.; Kishimoto, S.; Maruyama, S.; Mizutani, T. *Phys. Status Solidi B* **2007**, *244*, 4002−4005.
(20) Silvera-Batista, C. A.; Wang, R. K.; Weinberg, P.; Ziegler, K. J. *Phys. Chem. Chem. Phys.* **2010**, *12*, 6990−6998.
(21) Fagan, J. A.; Huh, J. Y.; Simpson, J. R.; Blackburn, J. L.; Holt, J. M.; Larsen, B. A.; Hight Walker, A. R. *ACS Nano* **2011**, *5*, 3943−3953.
(22) McDonald, T. J.; Engtrakul, C.; Jones, M.; Rumbles, G.; Heben, M. J. *J. Phys. Chem. B* **2006**, *110*, 25339−25346.
(23) Li, L. J.; Nicholas, R.; Deacon, R.; Shields, P. *Phys. Rev. Lett.* **2004**, *93*, 6−9.
(24) Kang, Y. K.; Lee, O.-S.; Deria, P.; Kim, S. H.; Park, T.-H.; Bonnell, D. A.; Saven, J. G.; Therien, M. J. *Nano Lett.* **2009**, *9*, 1414−1418.
(25) Deria, P.; Sinks, L. E.; Park, T.-H.; Tomezsko, D. M.; Brukman, M. J.; Bonnell, D. A.; Therien, M. J. *Nano Lett.* **2010**, *10*, 4192−4199.
(26) Park, J.; Deria, P.; Therien, M. J. *J. Am. Chem. Soc.* **2011**, *133*, 17156−17159.
(27) McDonald, T. J.; Jones, M.; Engtrakul, C.; Ellingson, R. J.; Rumbles, G.; Heben, M. J. *Rev. Sci. Instrum.* **2006**, *77*, 053104.
(28) Resch, U.; Eychmueller, A.; Haase, M.; Weller, H. *Langmuir* **1992**, *8*, 2215−2218.
(29) Fellah, S.; Ozanam, F.; Gabouze, N.; Chazalviel, J. N. *Phys. Status Solidi A* **2000**, *182*, 367−372.
(30) Marquis, R.; Greco, C.; Schultz, P.; Meunier, S.; Mioskowski, C. *J. Nanosci. Nanotechnol.* **2009**, *9*, 6777−6782.
(31) Forney, M. W.; Poler, J. C. *J. Phys. Chem. C* **2011**, *115*, 10531−10536.
(32) O'Connell, M. J.; Bachilo, S. M.; Huffman, C. B.; Moore, V. C.; Strano, M. S.; Haroz, E. H.; Rialon, K. L.; Boul, P. J.; Noon, W. H.; Kittrell, C.; Ma, J.; Hauge, R. H.; Weisman, R. B.; Smalley, R. E. *Science* **2002**, *297*, 593−596.
(33) Strano, M. S.; Huffman, C. B.; Moore, V. C.; O'Connell, M. J.; Haroz, E. H.; Hubbard, J.; Miller, M.; Rialon, K.; Kittrell, C.; Ramesh, S.; Hauge, R. H.; Smalley, R. E. *J. Phys. Chem. B* **2003**, *107*, 6979−6985.
(34) Gutmann, V. *Electrochim. Acta* **1976**, *21*, 661−670.
(35) Engtrakul, C.; Davis, M. F.; Gennett, T.; Dillon, A. C.; Jones, K. M.; Heben, M. J. *J. Am. Chem. Soc.* **2005**, *127*, 17548−17555.
(36) Mistry, K. S.; Larsen, B. A; Bergeson, J. D.; Barnes, T. M.; Teeter, G.; Engtrakul, C.; Blackburn, J. L. *ACS Nano* **2011**, *5*, 3714−3723.
(37) Taha, A.; Mahmoud, M. M. *New J. Chem.* **2002**, *26*, 953−957.
(38) Bachilo, S. M.; Strano, M. S.; Kittrell, C.; Hauge, R. H.; Smalley, R. E.; Weisman, R. B. *Science* **2002**, *298*, 2361−2366.
(39) Sato, K.; Saito, R.; Jiang, J.; Dresselhaus, G.; Dresselhaus, M. S. *Phys. Rev. B* **2007**, *76*, 195446.
(40) Boxer, S. G. *The Photosynthetic Reaction Center*; Academic Press: New York, 1993; Vol. *2*, pp 179−220.
(41) Liptay, W. *Excited States*; Academic Press: New York, 1974; Vol. *1*, pp 129−229.
(42) Suppan, P. *J. Photochem. Photobiol., A* **1990**, *50*, 293−330.
(43) Bergin, S. D.; Sun, Z.; Rickard, D.; Streich, P. V.; Hamilton, J. P.; Coleman, J. N. *ACS Nano* **2009**, *3*, 2340−2350.
(44) Bergin, S. D.; Nicolosi, V.; Streich, P. V.; Giordani, S.; Sun, Z.; Windle, A. H.; Ryan, P.; Niraj, N. P. P.; Wang, Z. T. T.; Carpenter, L.; Blau, W. J.; Boland, J. J.; Hamilton, J. P.; Coleman, J. N. *Adv. Mater.* **2008**, *20*, 1876−1881.
(45) Hansen, C. M. *Ind. Eng. Chem. Prod. Res. Dev.* **1969**, *8*, 2−11.
(46) Barone, P. W.; Parker, R. S.; Strano, M. S. *Anal. Chem.* **2005**, *77*, 7556−62.
(47) Heller, D. A.; Jin, H.; Martinez, B. M.; Patel, D.; Miller, B. M.; Yeung, T.-kwan; Jena, P. V.; Höbartner, C.; Ha, T.; Silverman, S. K.; Strano, M. S. *Nat. Nanotechnol.* **2009**, *4*, 114−20.